Doubly resonant three-photon double ionization of Ar atoms induced by an EUV free-electron laser

Gryzlova, E. V.; Ma, Ri; Fukuzawa, H.; Motomura, K.; Yamada, A.; Ueda, K.; Grum-Grzhimailo, A. N.; Kabachnik, N. M.; Strakhova, S. I.; Rouzee, A.; Hundermark, A.; Vrakking, M. J. J.; Johnsson, Per; Nagaya, K.; Yase, S.; Mizoguchi, Y.; Yao, M.; Nagasono, M.; Tono, K.; Togashi, T.; Senba, Y.; Ohashi, H.; Yabashi, M.; Ishikawa, T.

Published in:
Physical Review A (Atomic, Molecular and Optical Physics)

DOI:
10.1103/PhysRevA.84.063405

2011

Doubly resonant three-photon double ionization of Ar atoms induced by an EUV free-electron laser

E. V. Gryzlova,[1,2] Ri Ma,[1,3,4] H. Fukuzawa,[1,3] K. Motomura,[1,3] A. Yamada,[1,3] K. Ueda,[1,3,*] A. N. Grum-Grzhimailo,[2] N. M. Kabachnik,[2,5] S. I. Strakhova,[2] A. Rouzée,[3,6,7] A. Hundermark,[3,6,7] M. J. J. Vrakking,[6,7] P. Johnsson,[3,8] K. Nagaya,[3,9] S. Yase,[3,9] Y. Mizoguchi,[3,9] M. Yao,[3,9] M. Nagasono,[3] K. Tono,[3] T. Togashi,[3,10] Y. Senba,[3,10] H. Ohashi,[3,10] M. Yabashi,[3] and T. Ishikawa[3]

[1]*Institute of Multidisciplinary Research for Advanced Materials, Tohoku University, Sendai 980-8577, Japan*
[2]*Institute of Nuclear Physics, Moscow State University, Moscow 119991, Russia*
[3]*RIKEN, XFEL Project Head Office, Sayo, Hyogo 679-5148, Japan*
[4]*Institute of Atomic and Molecular Physics, Jilin University, Changchun 130012, China*
[5]*European XFEL GmbH, D-22761 Hamburg, Germany*
[6]*Max-Born-Institut, Max-Born Straße 2A, D-12489 Berlin, Germany*
[7]*FOM Institute AMOLF, NL-1098 XG Amsterdam, Netherlands*
[8]*Department of Physics, Lund University, Post Office Box 118, SE-22100 Lund, Sweden*
[9]*Department of Physics, Kyoto University, Kyoto 606-8502, Japan*
[10]*Japan Synchrotron Radiation Research Institute, Sayo, Hyogo 679-5198, Japan*

(Received 8 July 2011; published 5 December 2011)

A mechanism for three-photon double ionization of atoms by extreme-ultraviolet free-electron laser pulses is revealed, where in a sequential process the second ionization step, proceeding via resonant two-photon ionization of ions, is strongly enhanced by the excitation of ionic autoionizing states. In contrast to the conventional model, the mechanism explains the observed relative intensities of photoelectron peaks and their angular dependence in three-photon double ionization of argon.

DOI: 10.1103/PhysRevA.84.063405 PACS number(s): 32.80.Fb, 32.80.Rm, 32.80.Zb

I. INTRODUCTION

Nonlinear processes in the interaction of extreme-ultraviolet (EUV) and x-ray intense pulses with isolated atoms have a fundamental importance for understanding the interaction of strong high-frequency fields with molecules, clusters, surfaces, and solids. Their investigation was boosted by the appearance of free-electron lasers (FELs) in the EUV and x-ray frequency range. The simplest nonlinear processes, two- and three-photon ionization of atoms, have attracted increasing attention since they provide a way to study the mechanisms of the nonlinear response of atoms in intense EUV and x-ray fields [1–5].

Although autoionization structures dominate the cross sections in weak-field photoionization as well as in the reverse process of dielectronic recombination, the autoionization mechanism so far has not been considered in the multiphoton multiple ionization processes nowadays studied using FELs. As the presence of autoionizing states (AISs) strongly modifies the photoelectron energy and angular distributions from single-photon ionization, one can expect them to also play a significant role for multiphoton processes. In this article, we demonstrate the importance of AIS for multiphoton ionization in the EUV range, using a specific example of resonantly enhanced three-photon double ionization (3PDI) of Ar from a recent study by means of photoelectron spectroscopy [6–8].

The 3PDI can be considered as a three-step process: (a) atomic ionization, (b) ionic excitation, and (c) ionization of the excited ion. In particular, in argon it proceeds via the following path:

$$\text{(a)}\ h\nu_1 + \mathrm{Ar}\ 3p^6\ {}^1S \rightarrow \mathrm{Ar}^+\ 3p^5\ {}^2P + e_1,$$

$$\text{(b)}\ h\nu_2 + \mathrm{Ar}^+\ 3p^5\ {}^2P \rightarrow \mathrm{Ar}^{+*}\ 3p^4({}^3P, {}^1D, {}^1S)n\ell\ {}^2L_J,$$

$$\text{(c)}\ h\nu_3 + \mathrm{Ar}^{+*}\ 3p^4({}^3P, {}^1D, {}^1S)n\ell\ {}^2L_J \rightarrow \mathrm{Ar}^{2+}\ 3p^4\ {}^3P, {}^1D, {}^1S + e_2,$$

where $L(J)$ is the orbital (total) angular momentum of the intermediate excited ionic $(\mathrm{Ar}^+)^*$ state and the photons $h\nu_1$, $h\nu_2$, $h\nu_3$ from the same FEL pulse are equivalent. At photon energies around 21 eV, where the experiments [7,8] have been performed, the 3PDI proceeds via the intermediate discrete ionic excited states $(\mathrm{Ar}^+)^*\ 3p^4({}^1D)3d$. Note that here and in the following the term of the core configuration is used only as a label. It indicates the dominant term in the wave function of the strongly mixed ionic state. Photoionization of the intermediate state at step (c) leads to the three states ${}^3P$, ${}^1D$, and ${}^1S$ of the final Ar^{2+} ion. The relative intensity of the corresponding photoelectron lines varies strongly with the photon energy, showing an anomalously strong ${}^1S$ peak [7,8]. This contradicts the conventional description of 3PDI where the last step (c) is considered as a direct photoionization of the intermediate state and where the ${}^1S$ peak is much weaker than two others (see below).

The observed spectra can be explained by accounting for resonance ionization via the excitation and decay of AIS in Ar^+. Then the above step (c) (for $n\ell = 3d$) is modified by the autoionization

$$\text{(c}')\ h\nu_3 + \mathrm{Ar}^{+*}\ 3p^4({}^3P, {}^1D, {}^1S)\,3d\ {}^2L_J \rightarrow \mathrm{Ar}^{+**}\ 3p^3n_1\ell_1n_2\ell_2 \rightarrow \mathrm{Ar}^{2+}\ 3p^4\ {}^3P, {}^1D, {}^1S + e_2,$$

leading to the "doubly resonantly enhanced" mechanism of 3PDI, as shown in Fig. 1 (compare to Fig. 2(b) of Ref. [7]). The notation $(\mathrm{Ar}^+)^{**}\ 3p^3n_1\ell_1n_2\ell_2$ represents the set of AISs located in the energy region of interest with strongly mixed configurations $3p^3(3d^2,3d4d,3d4s)$ and others. The

*ueda@tagen.tohoku.ac.jp

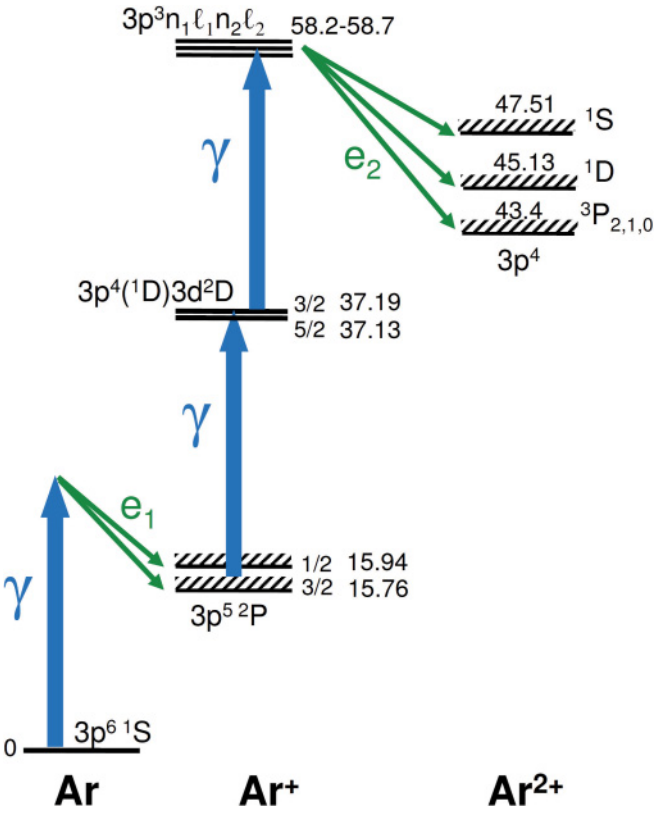

FIG. 1. (Color online) Scheme of doubly resonantly enhanced three-photon double ionization of Ar by FEL ($h\nu = 21.3$ eV). The energy levels in electron volts [9] are counted from the ground state of Ar.

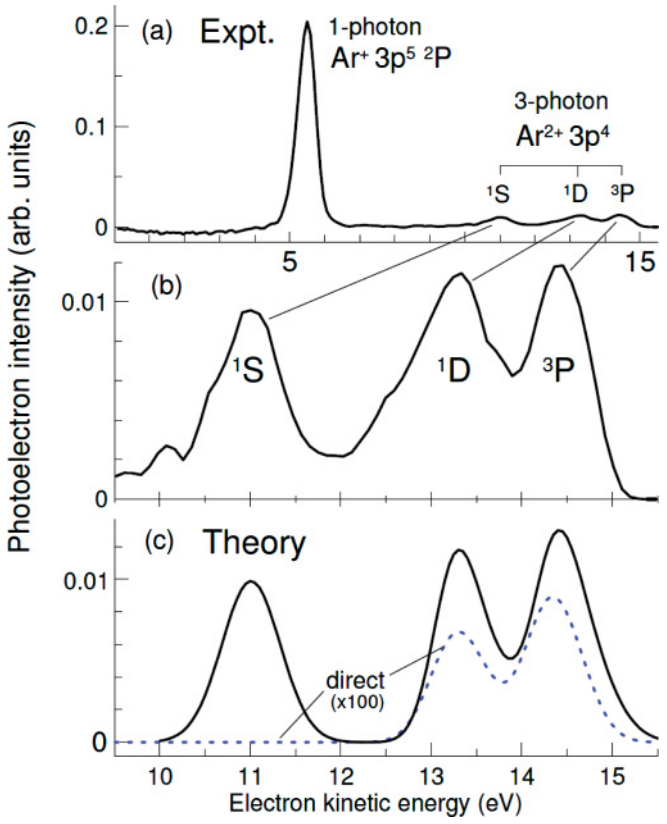

FIG. 2. (Color online) Measured [(a) and (b)] and calculated (c) angle integrated electron spectra at $h\nu = 21.3$ eV. Theory: Double resonant mechanism including AIS (solid) and without AIS, multiplied by 100 (dotted). The calculated spectra are convoluted with the Gaussian (FWHM = 0.45 eV); the peak positions are shifted to match the experiment.

dipole transition probabilities to these configurations from the intermediate $(Ar^+)^*\ 3p^4 3d$ state are very large when the photon energy matches the energy of a particular transition. Therefore, one can expect that the mechanism contributes significantly to the 3PDI, modifying the electron spectrum. Besides, involving AIS can lead to dramatic variations in the angular distribution of the photoelectrons in comparison with direct photoionization [10,11] since at resonance the relative weights and phases of the partial waves involved are determined by the properties (quantum numbers) of the AIS.

II. THEORY

To provide consistent theoretical predictions for the relative intensity of the photoelectron lines and the angular distribution of photoelectrons, we carried out extensive multiconfiguration Hartree-Fock (MCHF) calculations [12] of energies, oscillator strengths, photoionization and autoionization amplitudes, and alignment of intermediate ionic states. Our description is based on the density matrix and statistical tensor formalism [13] and extends our previous studies of sequential two-photon double ionization of noble gas atoms [14,15].

We consider the photon energies 21.3 and 21.45 eV in resonance with the transition $Ar^+\ 3p^5 \rightarrow Ar^{+*}\ 3p^4(^1D)3d\ ^2D$. The FEL spectrum varies from shot to shot, with the resulting spectrum covering an energy range of a few hundred millielectron volts. Therefore the doublet $3p^4(^1D)3d\ ^2P$ is also weakly excited. The first ionization step (a) is treated within the frozen-core MCHF model similar to the primary ionization in the sequential two-photon double ionization of Ar [15]. Thus, the relative populations of the $Ar^+(3p^5)^2P_{1/2,3/2}$ fine structure states and the alignment of the $Ar^+(3p^5)^2P_{3/2}$ state after the primary ionization are known. The second step (b) results in excited and polarized intermediate resonant doublets $Ar^{+*}3p^4(^1D)3d\ ^2D_J$ and ^2P_J. The transition probabilities and the alignment for the excitation from $Ar^+(3p^5)\ ^2P_{1/2,3/2}$ were calculated within the MCHF intermediate coupling approach taking into account the $3p^4n\ell\ (n \leqslant 6; \ell = s,d) + 3s3p^5(4p + 5p)$ configuration mixing. We assume that the fine structure levels are excited incoherently and model the FEL intensity envelope by a Gaussian with FWHM = 0.35 eV, thus weighting contributions from the intermediate $Ar^{+*}3p^4(^1D)3d\ ^2D_J, ^2P_J$ states.

Levels of the $(Ar^+)^{**}\ 3p^3n_1\ell_1n_2\ell_2$ configurations, excited at the third step (c), span a broad energy interval, which includes the region of the Ar^+ continuum. Spectroscopic data for the doubly excited $(Ar^+)^{**}\ 3p^3n_1\ell_1n_2\ell_2$ states are scarce [16] and relate to the lower part of the spectrum, while information on the higher lying AIS with an excitation energy of 21.0–21.8 eV from the $(Ar^+)^*\ 3p^4(^1D)3d\ ^2D, ^2P$ states, is needed for our purposes. Energies of the AIS $(Ar^+)^{**}$ with odd parity, as obtained from the MCHF calculations with 21 configurations of the type $3s^23p^3n_1\ell_1n_2\ell_2$ and $3s3p^5n_3\ell_3$,

TABLE I. Odd autoionizing states $3p^3 n_1\ell_1 n_2\ell_2$ of Ar^+ excited from Ar^+ $3p^4(^1D)3d\ ^2D_{3/2,5/2}$.[a]

N	Autoionizing state leading configurations	Term	E (eV)[b]	$A^c_{3/2}$ (units of c^{-1})	$A^c_{5/2}$ (units of c^{-1})	Γ^d (eV)	Branching[d], % ^1S	^3P	^1D
1	$42\%3p^3\ ^2D\ 3d\ ^1D\ 4s + 14\%3p^3\ ^2P\ 3d\ ^1D\ 4s + 5\%3p^3\ ^4S\ 3d\ ^3D\ 5d$	$^2D_{5/2}$	58.75	1.82[8]	1.04[8]	0.1	0	24	76
2	$26\%3p^3\ ^2D\ (3d^2\ ^1G) + 18\%3p^3\ ^2D\ 3d\ ^3G\ 4d + 18\%3p^3\ ^2P\ (3d\ ^3F)$	$^2G_{7/2}$	58.56		1.8[8]	0.22	9	0	91
3	$25\%3p^3\ ^2D\ (3d^2\ ^1G) + 21\%3p^3\ ^2P\ (3d^2\ ^1G) + 10\%3p^3\ ^2D\ 3d^2G\ 4d$	$^2F_{7/2}$	58.48		5.5[8]	0.20	76	11	14
4		$^2F_{5/2}$	58.40	5.6[8]	5.7[7]	0.19	82	18	0
5	$25\%3p^3\ ^2D\ 3d^1S\ 4d + 14\%3p^3\ ^2P\ (3d^2\ ^1G) + 11\%3p^3\ ^2P\ (3d^2\ ^1D)$	$^2D_{3/2}$	58.22	1.4[8]	5.7[6]	0.11	0	54	46
6		$^2D_{5/2}$	58.21	3.3[5]	2.5[8]	0.06	0	98	1
7	$26\%3p^3\ ^2P\ (3d^2\ ^1G) + 18\%3p^3\ ^2D\ 3d^1G\ 4d + 18\%3p^3\ ^2P\ (3d^2\ ^1D)$	$^2F_{5/2}$	58.18	1.2[8]	2.1[7]	0.13	39	25	36

[a]A few AISs with lower photoexcitation probability from $(Ar^+)^*\ 3p^4(^1D)3d\ ^2D, ^2P$ states are skipped.
[b]Energies are counted from the ground state of Ar atom; the calculated energy scale is normalized to spectroscopic data [9] at the energy of the state $Ar^{2+}\ 3s3p^5\ ^3P$ (57.56 eV).
[c]Transition rate between AIS and discrete $Ar^+\ 3p^4(^1D)3d\ ^2D_{3/2,5/2}$ states. Powers of 10 are indicated in square brackets.
[d]Decay width into $Ar^{2+}\ 3p^4$ multiplet and branching ratio into the multiplet states $3p^4\ ^1S, ^1D, ^3P$.

are summarized in Table I together with the relevant transition rates, decay widths, and branching ratios. Only those AISs are shown which are effectively excited from the intermediate states. The natural widths of the AISs are much larger than their fine-structure splitting.

The calculations show that due to the strong $3p \rightarrow 3d,4s,4d$ one-electron transitions, the probability of excitation of the AISs presented in Table I is much larger than the probability of direct photoionization from the $Ar^{+*}3p^4(^1D)3d\ ^2L$ states: in the ionization cross section, the autoionizing resonances should appear as strong lines on a negligibly weak background of direct ionization. When calculating the relative intensities of the photoelectron lines and the angular distributions of the photoelectrons e_2, we accounted for polarization of the intermediate AIS after the photoabsorption. The angular distribution takes the form

$$W(E_e,\vartheta) = \frac{W_0(E_e)}{4\pi}\left[1 + \sum_{k=2}^{k_{\max}} \beta_k(E_e) P_k(\cos\vartheta)\right], \qquad (1)$$

where $W_0(E_e)$ is the angle-integrated intensity, $\beta_k(E_e)$ ($k =$ even) are anisotropy parameters at electron (e_2) kinetic energy E_e, $P_k(x)$ is the Legendre polynomial of order k, and ϑ is the polar angle with respect to the laser polarization axis. An overlap of the closely located AISs due to their natural widths (see Table I) leads to the interference of the AISs, which was taken into account according to [17]. For the absorption of three linearly polarized photons, $k_{\max} = 6$, and is additionally restricted for different parts of the electron spectrum by the values of the angular momenta of the involved interfering AIS. Decay of the AIS into the $Ar^{2+}\ 3s3p^5\ ^3P$ (57.60 eV) hole state is not essential: the low-energy electron spectrum around 1 eV does not contain the corresponding lines (see below) and our calculations confirm this statement.

III. EXPERIMENT

To validate the above theoretical analysis, we have performed experiments using the Spring-8 Compact SASE Source (SCSS) test accelerator in Japan. The FEL light source provided EUV pulses with a temporal width of ~100 fs at a repetition rate of 30 Hz. The photon energies were set to 21.3 and 21.45 eV. The FEL beam was steered by two upstream SiC plane mirrors, passed a gas monitor detector (GMD) that measured the laser power, and then entered the prefocusing system of the beam line. The GMD was calibrated using a cryogenic radiometer [18]. The average pulse energy measured by the GMD during our experiment was 10.5 μJ with a standard deviation of 3.7 μJ. The focusing system consisted of a pair of elliptical and cylindrical mirrors coated with SiC. The total reflectivity of the 1-m focal length focusing system was 70%. Before entering the interaction chamber, the FEL beam passed through two sets of light baffles, each consisting of three skimmers with 4 mm and 3 mm diameters, respectively. These baffles successfully removed

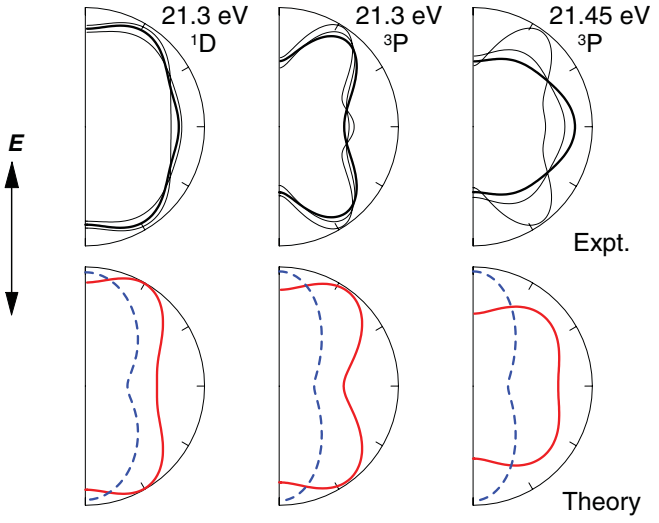

FIG. 3. (Color online) Measured (upper) and calculated (lower) angular distributions of electrons in the 3PDI. Experiment: at the maxima of the photoelectron lines (bold) and at energies shifted by ±0.1 eV from the maxima (thin). The theoretical curves are denoted as in Fig. 2(c) and correspond to the maxima of the photoelectron lines. The final Ar^{++} term and the photon energy are indicated for each column. Direction of the FEL polarization $\boldsymbol{E}$ is shown.

the majority of the scattered light that was specularly and nonspecularly reflected by the two mirrors. The skimmed FEL beam was focused onto an atomic beam at the center of a velocity map imaging spectrometer. The ~25-μm spot size diameter that was estimated in our experiment [19] results in an average intensity of $\sim 1.5 \times 10^{13}$ W/cm^2. Electrons produced by photoionization of the atoms by the FEL light were accelerated toward a position-sensitive detector consisting of a set of microchannel plates (MCPs) followed by a phosphor screen and recorded using a CCD camera synchronized to the arrival of the FEL pulse in the interaction chamber. A 200-ns electrical gate pulse was applied to the back of the MCPs in order to suppress the influence of dark counts on the detector. The measured two-dimensional (2D) projection allows the three-dimensional (3D) momentum distribution of the ejected electrons to be obtained using a mathematical inversion procedure. The retrieved 3D momentum distribution at each electron energy was fitted by Eq. (1).

IV. DISCUSSION

Figures 2(a) and 2(b) show a typical photoelectron spectrum with the main photoelectron line at an electron energy of ~5.5 eV from the single photoionization (first step) and a part corresponding to the three-photon double ionization to the ground-state multiplet $3p^4(^1S, ^1D, ^3P)$ of the ion Ar^{2+} at higher energies. Note that we expect the ^1D line to be perturbed by the direct two-photon single ionization $2h\nu + \mathrm{Ar}\, 3s^2 3p^6 \rightarrow \mathrm{Ar}^+ 3s3p^6 + e$ [7]. The ^1S line is as strong as the two other lines, which is in accordance with the measurements [7] at $h\nu = 21.2$–21.4 eV integrated over the electron emission angle. This line is even stronger in the experiments [8] at $h\nu = 21.4$ eV and 21.65 eV under the angle $\vartheta = 0^\circ$. Only taking the AIS into consideration allows us to obtain good agreement with the measurements [Figs. 2(b) and 2(c)]. Ionization without accounting for the AIS provides a negligible ^1S photoelectron line, in contradiction with the measured spectra.

The angular distributions of the photoelectrons are a further critical test for the analysis of the 3PDI mechanism. Again, as illustrated by Fig. 3, the angular distributions can be reproduced only when the AISs are included irrespective of a variety of electron wave functions and set of configurations tested. Moreover, as is seen from the right two columns of Fig. 3, small variation of the photon energy (only 0.15 eV) leads to a noticeable change of the experimental angular distribution. Excitation of AIS naturally explains this striking fact, since a small shift in energy means excitation of another resonance which can have completely different angular distribution. Our calculations reproduce well the experimental data.

In conclusion, by a joint theoretical and experimental study of the ionization of Ar by intense EUV radiation from a FEL, we have revealed the crucial role of AIS in multiphoton ionization and established an important new mechanism of producing doubly charged ions: doubly resonantly enhanced three-photon double ionization involving ionic autoionizing states.

ACKNOWLEDGMENTS

We are grateful to the SCSS Test Accelerator Operation Group at RIKEN for continuous support in the course of the studies and to the staff of the technical service section in IMRAM, Tohoku University, for their assistance in constructing the apparatus. This study was supported by the X-ray Free Electron Laser Utilization Research Project of the Ministry of Education, Culture, Sports, Science, and Technology of Japan, by the Japan Society for the Promotion of Science, and by the IMRAM project. E.V.G., A.N.G., N.M.K., and S.I.S. acknowledge support by the Russian Foundation for Basic Research. P. J. acknowledges support from the Swedish Research Council and the Swedish Foundation for Strategic Research.

[1] R. Moshammer *et al.*, Phys. Rev. Lett. **98**, 203001 (2007).
[2] A. A. Sorokin, S. V. Bobashev, T. Feigl, L. Tiedtke, H. Wabnitz, and M. Richter, Phys. Rev. Lett. **99**, 213002 (2007).
[3] M. Richter, M. Y. Amusia, S. V. Bobashev, T. Feigl, P. N. Juranic, M. Martins, A. A. Sorokin, and K. Tiedtke, Phys. Rev. Lett. **102**, 163002 (2009).
[4] M. G. Makris, P. Lambropoulos, and A. Mihelič, Phys. Rev. Lett. **102**, 033002 (2009).
[5] N. Berrah *et al.*, J. Mod. Opt. **57**, 1015 (2010).
[6] H. Fukuzawa *et al.*, J. Phys. B **43**, 111001 (2010).
[7] Y. Hikosaka *et al.*, Phys. Rev. Lett. **105**, 133001 (2010).
[8] N. Miyauchi *et al.*, J. Phys. B **44**, 071001 (2011)
[9] NIST Atomic Spectra Database (version 5.1.4), [http://physics.nist.gov/asd3].
[10] D. Dill, Phys. Rev. A **7**, 1976 (1973).
[11] N. M. Kabachnik and I. P. Sazhina, J. Phys. B **9**, 1681 (1976).
[12] C. Froese Fischer, T. Brage, and P. Jönsson, *Computational Atomic Structure: An MCHF Approach* (IOP Publishing, Bristol, 1997).
[13] V. V. Balashov, A. N. Grum-Grzhimailo, and N. M. Kabachnik, *Polarization and Correlation Phenomena in Atomic Collisions: A Practical Theory Course* (Kluwer Plenum, New York, 2000).
[14] M. Kurka *et al.*, J. Phys. B **42**, 141002 (2009).
[15] S. Fritzsche, A. N. Grum-Grzhimailo, E. V. Gryzlova, and N. M. Kabachnik, J. Phys. B **41**, 165601 (2008); **42**, 145602 (2009).
[16] F. Combet-Farnoux, P. Lablanquie, J. Mazeau, and A. Huetz, J. Phys. B **33**, 1597 (2000).
[17] M. Kitajima *et al.*, J. Phys. B **34**, 3829 (2001).
[18] M. Kato *et al.*, Nucl. Instrum. Methods Phys. Res., Sect. A **612**, 209 (2009).
[19] H. Ohashi *et al.*, Nucl. Instrum. Methods Phys. Res., Sect. A **649**, 163 (2011).